ELSEVIER

Marine Chemistry 80 (2002) 11–26

MARINE CHEMISTRY

www.elsevier.com/locate/marchem

Calibration of sediment traps and particulate organic carbon export using ^{234}Th in the Barents Sea

L. Coppola [a,*], M. Roy-Barman [a,b], P. Wassmann [c], S. Mulsow [d], C. Jeandel [a]

[a] *LEGOS, 14 av. E. Belin, 31400 Toulouse, France*
[b] *LSCE, Avenue de la Terrasse, 91198 Gif sur Yvette, France*
[c] *Norwegian College of Fishery Science, University of Tromsø, N-9037 Tromsø, Norway*
[d] *MEL-IAEA, 4 quai Antoine I B.P.800, MC 98000, Monaco, France*

Received 22 May 2001; received in revised form 27 June 2002; accepted 3 July 2002

Abstract

Profiles of particulate and dissolved ^{234}Th ($t_{1/2} = 24.1$ days) in seawater and particulate ^{234}Th collected in drifting traps were analyzed in the Barents Sea at five stations during the ALV3 cruise (from June 28 to July 12, 1999) along a transect from 78°15′N–34°09′E to 73°49′N–31°43′E. ^{234}Th/^{238}U disequilibrium was observed at all locations. ^{234}Th data measured in suspended and trapped particles were used to calibrate the catchment efficiency of the sediment traps. Model-derived ^{234}Th fluxes were similar to ^{234}Th fluxes measured in sediment traps based on a steady-state ^{234}Th model. This suggests that the sediment traps were not subject to large trapping efficiency problems (collection efficiency ranges from 70% to 100% for four traps). The export flux of particulate organic carbon (POC) can be calculated from the model-derived export flux of ^{234}Th and the POC/^{234}Th ratio. POC/^{234}Th ratios measured in suspended and trapped particles were very different (52.0 ± 9.9 and 5.3 ± 2.2 μmol dpm^{-1}, respectively). The agreement between calculated and measured POC fluxes when the POC/^{234}Th ratio of trapped particles was used confirms that the POC/^{234}Th ratio in trap particles is representative of sinking particles. Large discrepancies were observed between calculated and measured POC fluxes when the POC/^{234}Th ratio of suspended particles was used. In the Barents Sea, vertical POC fluxes are higher than POC fluxes estimated in the central Arctic Ocean and the Beaufort Sea and lower than those calculated in the Northeast Water Polynya and the Chukchi Sea. We suggest that the latter fluxes may have been strongly overestimated, because they were based on high POC/^{234}Th ratios measured on suspended particles. It seems that POC fluxes cannot be reliably derived from thorium budgets without measuring the POC/^{234}Th ratio of sediment trap material or of large filtered particles.

Keywords: Thorium-234; Sediment trap; POC export; Barents Sea

1. Introduction

Particle fluxes are usually measured by sediment traps to estimate particle abundance and particle sinking speed. Variations of the quantity and presumably of the quality of particulate matter (including

* Corresponding author. Tel.: +33-5-61-33-28-47; fax: +33-5-61-25-32-05.
E-mail address: coppola@notos.cst.cnes.fr (L. Coppola).

0304-4203/02/$ - see front matter © 2002 Elsevier Science B.V. All rights reserved.
PII: S0304-4203(02)00071-3

particulate organic carbon i.e. POC) recovered in a trap reflect the characteristics of the surface water dynamics and biomass composition. However, hydrodynamic effects and swimmers might seriously bias trapping efficiency (Buesseler, 1991; Gardner, 1996). Therefore, the use of traps alone is not sufficient to estimate correctly particle fluxes. Independent measurements of vertical flux from ^{234}Th activities in the water column can be used to calibrate the sediment trap catchment efficiency (Buesseler, 1991). This method is based on the fact that ^{238}U (half-life 4.5×10^9 years) has a conservative behavior in the ocean, whereas its daughter product, ^{234}Th (half-life $t_{1/2} = 24.1$ days), is highly particle-reactive and hence sticks to all particle surfaces. From the ^{234}Th deficiency (relative to ^{238}U) in surface waters, we can predict the particulate ^{234}Th flux exported from these waters (Coale and Bruland, 1985, 1987). By comparing this flux with ^{234}Th measurement in a trap, we can estimate if the trap collects ^{234}Th-bearing particles quantitatively (Gardner, 1996). The particulate organic carbon export can be derived if the ratio POC/^{234}Th is known. However, the relationships between POC and ^{234}Th are not well understood.

The Barents Sea is an arctic shelf sea of the eastern North Atlantic, which supports one of the most productive marine ecosystems in the Arctic region (Wassmann et al., 1999). The annual estimates of primary production range from 18 to 73 g C m^{-2} $year^{-1}$ between the northern and the southern part of the Barents Sea (Wassmann and Slagstad, 1993). This region is characterized by large regional differences in hydrographic conditions and ice coverage (Loeng, 1991; Loeng et al., 1997). Atlantic water flowing into the Barents Sea from south–west and Arctic water entering from north–east are separated by the Polar Front. The northern, central and eastern Barents Sea is periodically ice covered. The marginal ice zone (MIZ) is a unique frontal system (Wassmann et al., 1999). During late spring and early summer, the ice melt gives rise to a stratified and nutrient-rich euphotic zone. It is followed by a phytoplankton bloom (Slagstad and Wassmann, 1997). Temporal and spatial variability of vertical flux of biogenic matter is important to understand elemental dynamics and food webs in the ocean (Legendre, 1990; Smetacek et al., 1984; Wassmann, 1991). The dynamics of this flux and the composition of the exported production were investigated during previous studies along a section in the central Barents Sea during the 1984–1993 period (Wassmann and Slagstad, 1993). Along this south–north transect, the zonal structure of the Barents Sea with its main water masses (Atlantic water, the Polar Front, the ice edge and Arctic water) was investigated (Andreassen and Wassmann, 1998). Physical processes may also influence the dynamics of the vertical flux in the Barents Sea through their impact on ice coverage, ice melt, stabilization, advection and retention of zooplankton (Slagstad and Wassmann, 1997; Wassmann and Slagstad, 1993).

We present water column measurements of dissolved and particulate ^{234}Th and ^{234}Th collected in sediment traps at five stations representing different trophic features corresponding to different ice coverage conditions and different water masses (Arctic and Atlantic waters). These results are used to calibrate sediment traps, to quantify POC export in this region and to compare these estimates with direct POC export estimates.

2. Methods

2.1. Sample collection

Samples were collected onboard RV "Jan Mayen" from June 28, 1999 to July 12, 1999, during ALV3 cruise (Arctic Light and Heat), along a transect in the central Barents Sea. The sampling area was from 78°15′N–34°09′E to 73°49′N–31°43′E (Fig. 1). Heading for the north, we tried to penetrate as deep as possible into the MIZ. Along this south–north section, POC in small particles, nutrients and plankton were measured during short stations. When the northernmost station was reached (78°N), we realized five process-oriented long stations (e.g. vertical flux, fecal pellet production, etc.). The choice of these stations depended on the type of ice (close and open drift ice, i.e. stations 1 and 2, respectively) and the water mass (the PF/MIZ, north and south branches of the Atlantic water penetrating in the Barents Sea, i.e. stations 3, 4 and 5, respectively). During long stations, drifting sediment traps were deployed at several depths for 24 h.

At each station, seawater samples were taken at 10, 30, 50, 100 and 120–200 m (except at station 3

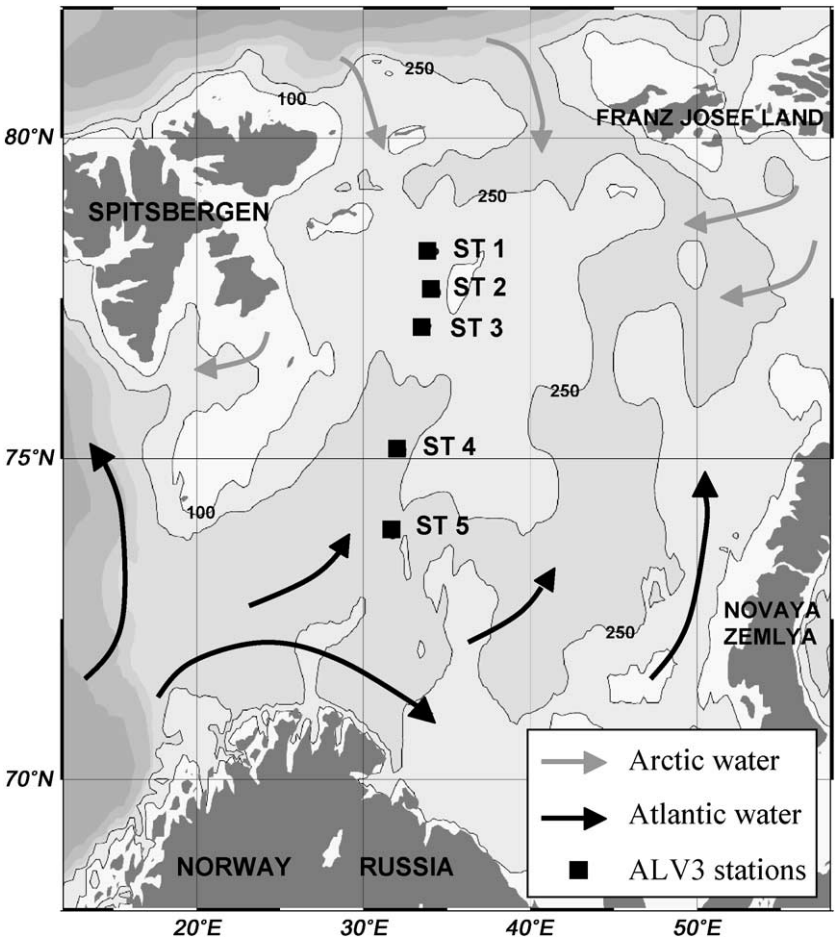

Fig. 1. Long stations location during the ALV3 cruise.

because the bottom was shallower than at other stations) with 5-l Niskin bottles to collect dissolved and particulate ^{234}Th. Sediment trap deployments were performed at five stations. A drifter with an array of sediments traps at eight depths (30, 40, 50, 60, 90, 120, 150, 200 m) was deployed to collect settling particles during 24 h. The sediment traps (KC maskiner og laboratorieudstyr, Denmark) were parallel cylinders mounted in a gimbaled frame equipped with a vane. The cylinders remain vertical and perpendicular to the currents direction. The cylinders were 0.072 m in diameter and 0.45 m high (H/D ratio 6.25). No bafflers were used on the cylinders and no poison was applied during the deployment. At each station, 50% of the material collected in the deepest trap (between 90 and 200 m) was recovered for ^{234}Th analyses.

2.2. ^{234}Th analyses

To measure particulate ^{234}Th in water column, 10 l of seawater was filtered through 142 mm diameter 0.6 μm pore size Nuclepore filters. The filtered water was used to measure the dissolved phase. It was acidified to pH 2 with 18 ml HCl 6 N (double distilled) and 40 mg of Fe carrier was added. As 100% recovery cannot be guaranteed, ^{229}Th was used as a yield tracer. The solution was mixed to homogenize and left to stand overnight for isotopic equilibration. Then, we used NH_3 (25%) to raise the pH to 8 to produce an iron

hydroxide precipitate that scavenges dissolved ^{234}Th and ^{229}Th (Roy-Barman et al., 1996). After waiting 24 h for particles to settle, the precipitate was recovered by filtration through another 0.6 μm Nuclepore filter. Trapped particles (with sediment traps) were filtered onto 0.6 μm pore size Nuclepore filter.

After 2 weeks, ^{234}Th was quantified using non-destructive beta counting techniques at the Marine Environment Laboratory of IAEA at Monaco. Filters were counted with a low-background (0.31 cpm) beta counter (Risø National Laboratory) following the procedure of Rutgers van der Loeff and Moore (1999). Before particulate and dissolved ^{234}Th measurements, the counter was calibrated with an ^{238}U standard. Blanks were measured for filter and iron precipitate. Counting time was a 10×100 min cycle for particulate ^{234}Th and 5×100 min cycle for dissolved ^{234}Th. The yield of the procedure was estimated by measuring the quantity of ^{229}Th present in the iron precipitate recovered by filtration. This precipitate was dissolved in HCl 6 N and a known amount of ^{232}Th was added to an aliquot of this solution. After isotopic equilibration, thorium isotopes were purified by ion exchange column chemistry (AG1X8). The ^{229}Th/^{232}Th ratio was measured by mass spectrometry (Roy-Barman et al., 1996). Another aliquot of iron precipitate was used to measure ^{238}U concentration by IPC-MS to take into account the effect of ^{238}U decay between the iron precipitation and the ^{234}Th counting ($\sim$ 15 days). This procedure induces an accuracy about 8% for total ^{234}Th activities as a result of uncertainties related to the contribution from U and Th isotopes analyzed.

2.3. Particulate organic carbon analyses

The filtration of water samples and sediment trap samples was carried out on precombusted Whatman GF/F glass fiber filters (25 mm and 0.7 μm pore size). Subsample volume ranged from 25 to 250 ml. After filtration, the filters were washed with 20 ml of distilled water to remove salt and stored in a freezer for particulate organic carbon analyses. The samples were dried at 60 °C. The filters were treated with fumes of concentrated HCl before analysis to remove carbonates. POC was quantified using a Leeman Lab 440 analyzer (Wassmann, 1991). Repeated blank analyses demonstrate that the POC concentrations are not biased by any contamination.

3. Results

3.1. Hydrography

The main water masses encountered along the transect are identified with the temperature section (Fig. 2a). Atlantic water was predominant in the south and in the center of the section. It was divided in two branches which penetrated the Barents Sea from the south–west. The South Barents Atlantic-derived Water (SBAW) was 4–7 °C while the North Barents Atlantic-derived Water (NBAW) was colder at 2–4 °C. On the Sentralbanken, a specific water mass (Sentralbanken Water i.e. SW) of Arctic origin was isolated between the SBAW and the NBAW with a temperature lower than 2 °C. The NBAW reached the MIZ at about 76.5°N. At this latitude, a strong temperature gradient was observed in the entire water column corresponding to the Polar Front and the start of the ice coverage. In the northern part of the transect, Arctic water (AW) was present with temperatures lower than 0 °C and salinities less than 34‰ in the upper layer due to ice melting.

3.2. Nutrients

The distribution of nitrate followed the hydrographic features described above (Fig. 2b). In the upper layer (0–50 m) of Atlantic water, a clear depletion of nutrients compared to the winter values was observed (higher than 10.4 μM in March; Reigstad et al., accepted for publication). This depletion was present from south to north of Sentralbanken. In deeper waters, nitrate concentrations were higher. Between 75°N and 76°N, the decrease of nutrients reflects the presence of NBAW. Beyond 77°N, the high nitrate concentration measured in the ice-covered waters indicates that light was too weak for a bloom to develop. The highest Chla concentration (measured along the ALV3 transect) was located just at the ice edge reflecting an ice-edge bloom while those under the ice were low and decreased toward the north. The low biomass present south of the ice edge in the melt water as well as the Atlantic waters is typical for summer (Reigstad et al., accepted for

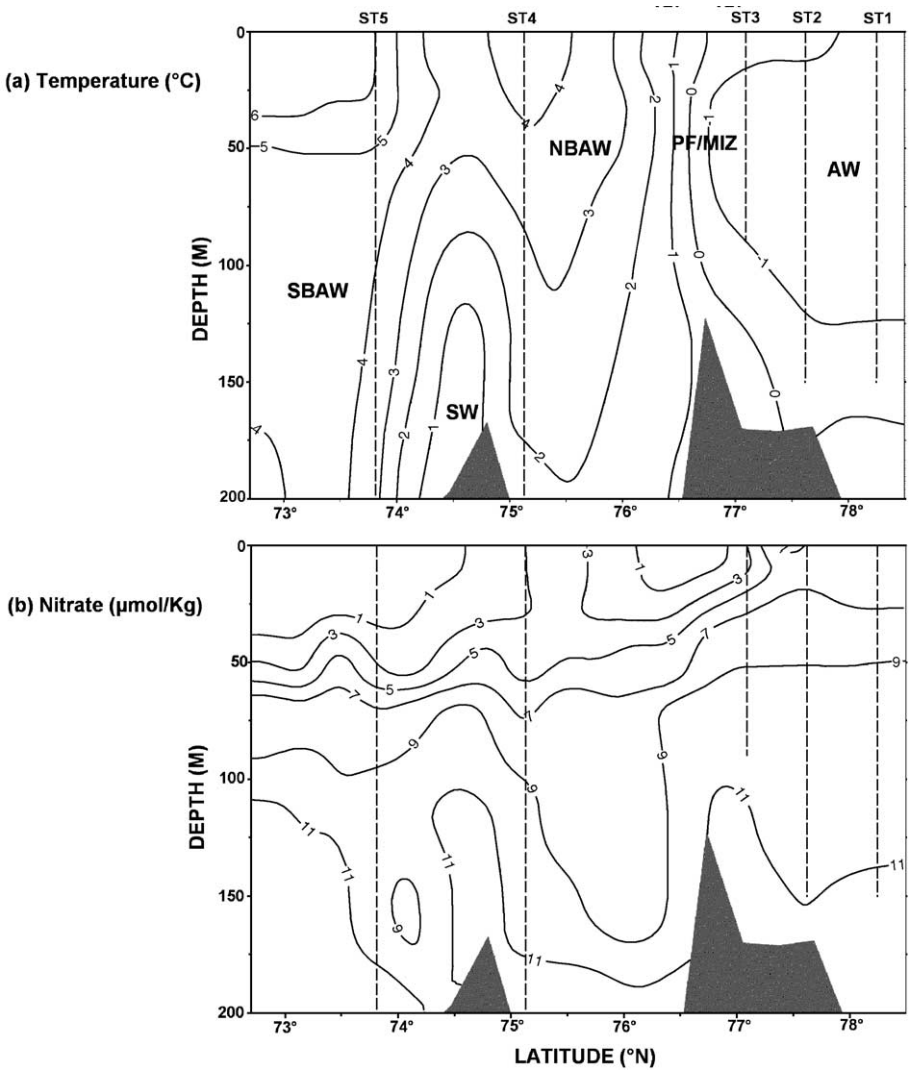

Fig. 2. Distribution of temperature and nitrate along the ALV3 transect. Temperature (°C) (SBAW = South Barents Atlantic derived Water; SW = Sentralbanken Water; NBAW = North Barents Atlantic derived Water; PF/MIZ = Polar Front/Marginal Ice Zone; AW = Arctic Water). Nitrate (µmol/kg).

publication). Previous cruises along the same transect and modeling work showed that the spring bloom in the MIZ takes place in April/June in the central Barents Sea (Wassmann et al., 1999). This suggests that the bloom had already happened in the Atlantic waters when the cruise took place.

3.3. ^{234}Th activities and POC concentrations

^{234}Th activities and POC concentrations are listed in Table 1 and depth profiles of ^{234}Th are shown in Fig. 3. ^{238}U activities were calculated from salinity using the relationship $^{238}U(\mathrm{dpm\ l^{-1}}) = 0.071 \times S(‰)$ (Chen et al., 1986). When total ^{234}Th activity (the sum of dissolved and particulate activities) in samples display values close to ^{238}U activity, this indicates that total ^{234}Th is in radioactive equilibrium with ^{238}U. Deviations from this equilibrium can reflect both scavenging or mineralization (Coale and Bruland, 1987). In the present study, ^{234}Th/^{238}U disequilibria are observed at all locations. At the northern stations (1, 2, 3), total ^{234}Th activities decrease between 0 and 50 m. The 50 m

Table 1
POC concentrations and ^{234}Th and ^{238}U activities in the Barents Sea, 1999

Water depth (m)	POC (μM)	Dissolved ^{234}Th <0.6 μm (dpm l^{-1})	Particulate ^{234}Th >0.6 μm (dpm l^{-1})	Total ^{234}Th (dpm l^{-1})	^{238}U (dpm l^{-1})	$^{234}Th/^{238}U$ (dpm/dpm)
St1 (#448, 78.25°N, 34.15°E, 180 m)						
10	15.16	1.45 ± 0.13	0.23 ± 0.02	1.68 ± 0.13	2.40	0.70 ± 0.06
30	12.45	1.61 ± 0.15	0.19 ± 0.02	1.80 ± 0.15	2.42	0.74 ± 0.06
50	8.25	1.00 ± 0.13	0.27 ± 0.02	1.27 ± 0.13	2.45	0.52 ± 0.05
100	5.89	1.78 ± 0.14	0.28 ± 0.02	2.06 ± 0.14	2.46	0.84 ± 0.06
150	5.70	1.33 ± 0.11	0.37 ± 0.03	1.70 ± 0.11	2.48	0.69 ± 0.05
St2 (#461, 77.62°N, 34.39°E, 197 m)						
10	19.56	1.59 ± 0.15	0.21 ± 0.02	1.80 ± 0.16	2.41	0.75 ± 0.06
30	12.87	1.49 ± 0.14	0.24 ± 0.02	1.73 ± 0.14	2.46	0.71 ± 0.06
50	10.16	1.42 ± 0.13	0.23 ± 0.02	1.65 ± 0.14	2.46	0.67 ± 0.06
100	11.94	1.42 ± 0.13	0.26 ± 0.02	1.68 ± 0.14	2.46	0.68 ± 0.06
150	8.36	1.67 ± 0.15	0.31 ± 0.02	1.98 ± 0.15	2.47	0.80 ± 0.06
St3 (#474, 77.09°N, 33.78°E, 149 m)						
10	19.74	1.67 ± 0.14	0.60 ± 0.05	2.27 ± 0.15	2.37	0.96 ± 0.06
20	17.87	1.31 ± 0.15	0.70 ± 0.06	2.01 ± 0.16	2.37	0.85 ± 0.07
40	9.64	1.83 ± 0.15	0.20 ± 0.02	2.03 ± 0.15	2.45	0.83 ± 0.06
60	–	1.55 ± 0.14	0.21 ± 0.02	1.76 ± 0.14	2.46	0.72 ± 0.06
90	8.46	1.90 ± 0.14	0.26 ± 0.02	2.16 ± 0.14	2.47	0.88 ± 0.06
St4 (#488, 75.13°N, 32.35°E, 249 m)						
10	31.20	0.69 ± 0.13	0.40 ± 0.03	1.08 ± 0.13	2.49	0.44 ± 0.05
30	25.25	0.77 ± 0.13	0.40 ± 0.03	1.16 ± 0.13	2.49	0.47 ± 0.05
50	17.06	0.46 ± 0.09	0.70 ± 0.04	1.16 ± 0.10	2.49	0.47 ± 0.04
100	10.83	1.19 ± 0.12	0.11 ± 0.02	1.30 ± 0.12	2.48	0.52 ± 0.05
150	7.53	1.38 ± 0.14	0.20 ± 0.02	1.59 ± 0.14	2.49	0.64 ± 0.06
200	8.39	2.86 ± 0.15	0.22 ± 0.02	3.08 ± 0.15	2.48	1.24 ± 0.06
St5 (#501, 73.81°N, 31.71°E, 336 m)						
10	23.25	0.77 ± 0.08	0.47 ± 0.03	1.24 ± 0.09	2.48	0.50 ± 0.04
30	21.72	0.82 ± 0.08	0.35 ± 0.02	1.17 ± 0.09	2.48	0.47 ± 0.04
50	15.40	1.54 ± 0.15	0.37 ± 0.03	1.90 ± 0.15	2.48	0.77 ± 0.06
100	10.68	1.32 ± 0.13	0.07 ± 0.01	1.39 ± 0.13	2.49	0.56 ± 0.05
200	6.38	1.66 ± 0.21	0.15 ± 0.02	1.81 ± 0.21	2.48	0.73 ± 0.08

minimum is most pronounced at station 1. At these three stations, total ^{234}Th activities increase at depth without reaching equilibrium. At the southern stations, the largest disequilibrium is observed at the "surface" and the total ^{234}Th activities increase with depth (it slightly exceeds equilibrium at station 4). The particulate ^{234}Th activities are low at the surface of stations 1 and 2 and slightly increase toward the bottom. At stations 3–5, there is a maximum of particles at the surface and lower values at depth.

The POC concentrations measured on suspended particles in the central Barents Sea during the cruise was higher in surface layer (12–25 μmol/l between 0 and 50 m) and decreased with depth (8–10 μmol/l). At the southern stations (4 and 5), the POC concentrations measured in the surface layer (0–50 m) were 35% higher than at the northern stations (1–3). In deep layer, these concentrations were more homogeneous.

3.4. Trapped material

During this cruise, ^{234}Th fluxes were measured in the deepest trap at each stations (90–200 m). The ^{234}Th fluxes range from 1814 to 4713 dpm m^{-2} day^{-1}. ^{234}Th fluxes were lower in Arctic water than in Atlantic water. The lowest flux was recorded in the

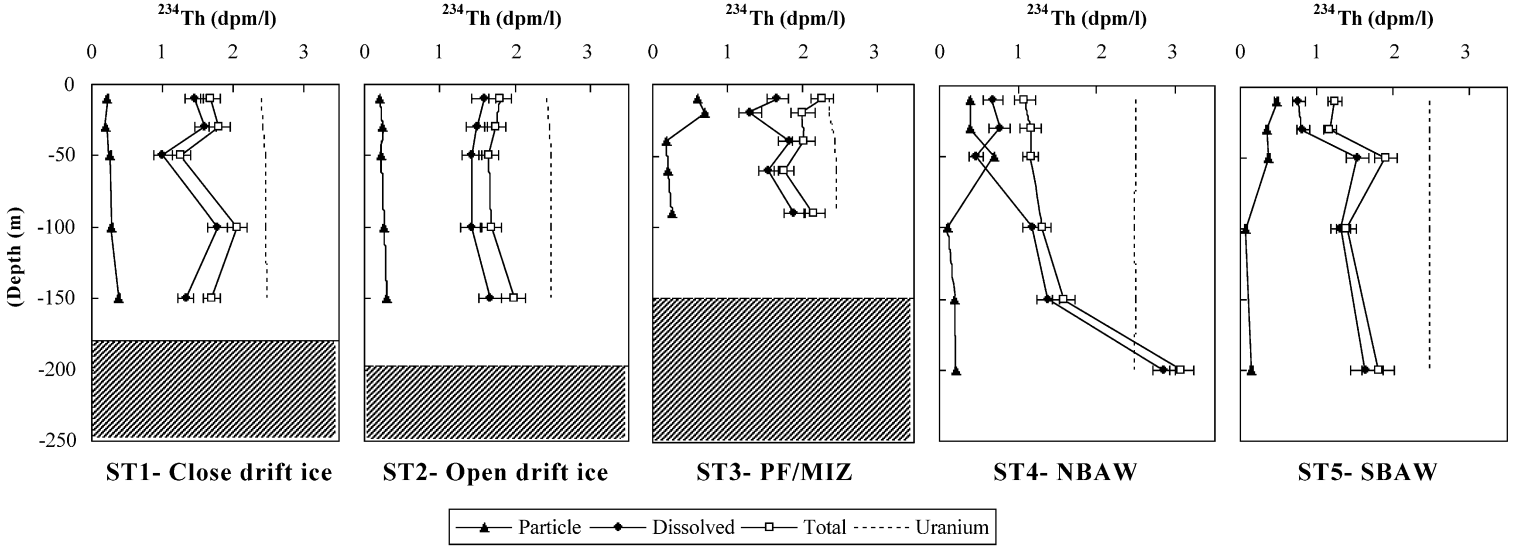

Fig. 3. Activity profiles of ^{234}Th in the Barents Sea (All activities are given in dpm l^{-1}).

Polar Front area (station 3). The latitudinal distribution of POC trap data was similar to the POC concentrations observed on suspended particles. The average of POC fluxes range from 145 to 180 mg C m^{-2} day^{-1} at the northern stations and from 240 to 320 mg C m^{-2} day^{-1} at the southern stations.

4. Discussion

4.1. Origins of $^{234}Th/^{238}U$ disequilibrium

As ^{234}Th is highly particle-reactive and sticks to all particle surfaces, the loss of ^{234}Th (i.e. $^{234}Th/^{238}U$ disequilibrium) from surface waters is a direct indication of the removal rate of sinking particulate matter. Coale and Bruland (1985) showed that there is a link between ^{234}Th removal rates and new production in the open ocean. However, other mechanisms can also explain a $^{234}Th/^{238}U$ disequilibrium. $^{234}Th/^{238}U$ disequilibrium throughout the water column has been previously observed in the Arctic region. In a continental shelf region of the NW Baltic Sea (Landsort Deep), a large $^{234}Th/^{238}U$ disequilibria about 0.5 was observed during spring/summer and probably related to spring bloom of diatoms (Andersson et al., 2000). In the Chukchi Sea, total $^{234}Th/^{238}U$ activity ratio as low as 0.14 was related to particle-rich shelf waters (Moran et al., 1997). In the Chukchi slope and Makarov Basin (the interior Arctic), total $^{234}Th/^{238}U$ activity ratios ranging from 0.6 to 0.9 were observed and attributed to local biological production. Results from the North Pole indicated no significant $^{234}Th/^{238}U$ disequilibrium (Moran et al., 1997). In the Beaufort Sea, the distribution of the total $^{234}Th/^{238}U$ activity ratio reveals a transition, centred at the shelf break, from low values (0.4–0.6) over the shelf to elevated ratios approaching a secular equilibrium (that is when the total ^{234}Th activity is equal to the ^{238}U activity) offshore (Moran and Smith, 2000). These results were explained by shelf scavenging and lateral transport (advection). In the Northeast Water Polynya, similar $^{234}Th/^{238}U$ activity ratios (0.6–1) were observed by Cochran et al. (1995). They were explained by resuspension of particles which could scavenge thorium at shallow depths.

In the present study, total $^{234}Th/^{238}U$ activity ratios ranged from 0.5 to 0.8 at the northern stations and from 0.4 to 1.2 at the southern stations. At stations located on the Spitsbergen Shelf, $^{234}Th/^{238}U$ ratios lower than 1 may be due to the intense scavenging (as observed in other shelf regions). In deeper waters, we suggest that $^{234}Th/^{238}U$ ratios higher than 1 (station 4) were due to the remineralization process. A striking aspect of these results is the $^{234}Th/^{238}U$ disequilibrium present throughout the water column at all stations except at station 4. We suggest that this may be due to the presence of high suspended POC concentrations caused by high biological production, inducing local scavenging throughout the water column. In the Barents Sea, POC concentrations measured in suspended matter are higher (they range from 6 to 30 μmol l^{-1}) than in other regions of the Arctic Ocean (0.1–5 μmol l^{-1}; Moran et al., 1997; Moran and Smith, 2000). It could explain the large disequilibrium of total ^{234}Th activities observed along the transect. Another additional scavenging mechanism may be the release of dead algae and sediments by the ice (Schubert and Calvert, 2001). However, this process was probably unimportant during this cruise: observation of the ice by divers indicated very little ‘‘dirty ice’’. This is consistent with the weak lateral transport that was unable to carry this ‘‘dirty ice’’ from the shelves.

We noted earlier that particle-rich shelf waters could be extremely depleted in ^{234}Th (Moran et al., 1997). We now evaluate if an advection of such ^{234}Th-depleted water mass from the Franz Josef Land to stations 1–3 can account for the $^{234}Th/^{238}U$ activity ratio observed at these stations ($\sim$ 0.8). Following Moran et al. (1997), we assume that the ^{234}Th depletion occurred in the Franz Josef Land vicinity ($^{234}Th/^{238}U \sim 0.2$ as observed in the Chukchi Shelf) and that the ^{234}Th particulate flux was negligible during the lateral transport so that the $^{234}Th/^{238}U$ activity ratio of the water mass evolves only by radioactive decay. In these conditions, 48 days ($2 \times t_{1/2}$ of ^{234}Th) is necessary to achieve the $^{234}Th/^{238}U$ disequilibrium observed at the northern stations ($^{234}Th/^{238}U = 0.8$). As the distance from the Franz Josef Land to stations 1–3 is of $\sim$ 400 km, an advective velocity of 9.6 cm s^{-1} is required to advect this water mass in 48 days. Geostrophic velocities were estimated with the θ-S data obtained during the cruise. At the northern stations, the mean current estimated between 0 and 3 cm s^{-1} was not sufficient

to explain the observed disequilibrium by advection of a water mass.

Horizontal eddy diffusion could contribute to $^{234}Th/^{238}U$ disequilibrium observed at the northern stations. Using the relationship of Okubo (1971), we calculate $K_h = 5.7 \times 10^6$ cm^2 s^{-1} for a length scale of 400 km. Using $t = 48$ days, the horizontal distance over the scavenging signature could travel before being obscured by ingrowth is $(K_h \times t)^{0.5} = 49$ km. This mechanism would generate a $^{234}Th/^{238}U$ disequilibrium of 0.8 (which is observed at the northern stations) at only 10% of the distance from Franz Josef Land and the system would have returned to equilibrium before the signal reaches station 1.

The net transport of water masses due to the tidal mixing in the central Barents Sea was calculated with a barotropic model (F. Lyard, personal communication). The strongest transport is located around the Norwegian coast, but in the central Barents Sea, the tidal mixing produces a speed current around 0.15 cm s^{-1}. This is clearly lower than the geostrophic velocities observed during the ALV3 cruise. Therefore, none of the stations was influenced by the tidal mixing.

The role of the sediment resuspension is difficult to constrain because neither the mineral content of the trapped material nor the bottom current velocity was measured during the cruise. However, if the sediment resuspension was important, we would expect an increase of the particulate thorium activities and the POC fluxes with depth at least close to the bottom. On the contrary, there is no significant near-bottom increase in the concentration of particulate thorium (there is a slight increase of particulate ^{234}Th at 200 m at station 5, but the seafloor is at 336 m depth). For the POC fluxes, we rather observe a decrease with depth (Olli et al., in press). Moreover, we note that sediment resuspension would influence our trap calibration only if the resuspended particles are young enough to still contain a substantial fraction of the ^{234}Th that they scavenged when they were first deposited (Bacon and Rutgers van der Loeff, 1989).

To conclude, it appears that horizontal transport did not participate significantly to the $^{234}Th/^{238}U$ disequilibrium. Based on the particulate thorium activities only, we will suppose that resuspended particles did not contribute to the ^{234}Th scavenging. Therefore, we suggest that the large presence of high POC concentrations (and thus POC export) observed during summer is the main cause of $^{234}Th/^{238}U$ disequilibria observed along the transect in the Barents Sea. In the following, this disequilibrium will be used to quantify the POC flux.

4.2. Determining ^{234}Th fluxes

We use a simple one-dimensional box model to estimate fluxes of dissolved ^{234}Th onto particles and of particulate ^{234}Th on sinking particles. In the water column, the source of ^{234}Th is the production from ^{238}U. The main sinks are radioactive decay and removal by scavenging on settling particles. The activity balance for dissolved and particulate ^{234}Th are given by Coale and Bruland (1985). Assuming a steady state and that the net effect of advective and diffusive transports of ^{234}Th are small compared to uptake of ^{234}Th on particles and radioactive decay (see Section 4.1), we calculate residence times for dissolved ^{234}Th (τ_d) and particulate ^{234}Th (τ_p):

$$\tau_d = \frac{A^d_{Th}}{J_{Th}} = \frac{A^d_{Th}}{\lambda(A_U - A^d_{Th})} \quad (1)$$

$$\tau_p = \frac{A^p_{Th}}{P_{Th}} = \frac{A^p_{Th}}{J_{Th} - A^p_{Th}\lambda} \quad (2)$$

where A_U is the ^{238}U activity, λ is the ^{234}Th decay constant (0.0288 day^{-1}), $A_{Th}{}^d$ and $A_{Th}{}^p$ are dissolved and particulate ^{234}Th integrated activities, respectively. The term J_{Th} (dpm m^{-2} day^{-1}) represents the net removal rate of dissolved ^{234}Th onto particles and P_{Th} (dpm m^{-2} day^{-1}) is the removal rate of particulate ^{234}Th on sinking particles.

For the quantification of ^{234}Th fluxes and residences times, we assume that the surface depletion is balanced by an export of ^{234}Th to deeper layers. In Table 2, we report data of ^{234}Th deficiencies, fluxes and residences times using trapezoidal integration of ^{234}Th depth profiles from 0 to 50 m and over the entire water column.

The removal rate of dissolved ^{234}Th (J_{Th}) and particulate ^{234}Th (P_{Th}) in the upper 50 m are in the range of $\sim$ 1100 and $\sim$ 600–900 dpm m^{-2} day^{-1}, respectively, in Arctic waters and $\sim$ 1730–2100 and $\sim$ 1280–1550 dpm m^{-2} day^{-1}, respectively, in

Table 2
Calculation of ^{234}Th deficiencies, fluxes and residence times

Station	Depth range (m)	^{234}Th deficit (10^3 dpm m^{-2})	J_{Th} (dpm m^{-2} day^{-1})	P_{Th} (dpm m^{-2} day^{-1})	τ_d (day)	τ_p (day)
St1	0–50	31.6 ± 3.5	1162 ± 97	909 ± 102	49 ± 5	10 ± 1
	0–150	100.8 ± 7.8	4016 ± 217	2903 ± 225	51 ± 3	13 ± 1
St2	0–50	28.7 ± 3.6	1094 ± 99	828 ± 104	55 ± 6	11 ± 2
	0–150	100.7 ± 8.2	3927 ± 229	2900 ± 236	53 ± 4	12 ± 1
St3	0–60	21.3 ± 4.5	1176 ± 114	614 ± 129	68 ± 7	32 ± 7
	0–90	36.4 ± 5.7	1816 ± 149	1050 ± 163	73 ± 7	25 ± 4
St4	0–50	53.8 ± 2.9	2093 ± 73	1549 ± 83	13 ± 1	12 ± 1
	0–200	176.3 ± 8.9	6739 ± 248	5079 ± 257	35 ± 2	12 ± 1
St5	0–50	44.4 ± 2.8	1725 ± 71	1279 ± 80	23 ± 2	12 ± 1
	0–200	174.9 ± 13.7	6121 ± 391	5037 ± 396	42 ± 4	7 ± 1

Atlantic waters. Particulate ^{234}Th fluxes exported from the upper 50 m are lower in Arctic waters than in Atlantic waters. Considering that the particulate fraction of ^{234}Th is associated with the phytoplankton in the surface water, the difference of particulate ^{234}Th fluxes reflects the ice cover, which limits the penetration of light, induces stratification and limits the supply of nutrients to the photic zone and the new production in Arctic waters (Luchetta et al., 2000).

In early spring, the entire northern Barents Sea is covered by ice and there are high concentrations of nutrients due to winter mixing. From March, the retreat of the ice edge, the opening of leads, the penetration of light through the ice and the stratification results in short bloom events characteristic for the MIZ (Falk-Petersen et al., 2000). At station 3 (located at the limit of ice edge), we note a strong gradient of nitrate in July (Fig. 2b). The strong vertical stability, the lack of horizontally advected water and the minor dilution by melt water support that changes in nutrient distribution can be associated mainly to biological activities (Luchetta et al., 2000). At station 3, a high POC content and a maximum of particulate ^{234}Th are observed. At this location, a *Phaeocystis pouchetii* bloom was observed and it was the only real bloom during the July cruise.

The residence time for dissolved ^{234}Th over the entire water column in Arctic and Atlantic waters ranges from 35 to 55 days but it is higher in the PF/MIZ region (~ 70 days). We find the same trend for particulate ^{234}Th. The residence time ranges from 7–13 days in Arctic and Atlantic waters to 25 days in the PF/MIZ. These results from Arctic and Atlantic waters are similar to those encountered in the Northeast Water Polynya (Cochran et al., 1995) and in the Beaufort Sea (Moran and Smith, 2000).

Irreversible scavenging is often described as a first-order process:

$$J_{Th} = k_1 \times A^{d}_{Th} \quad (3)$$

with:

$$k_1 = \frac{1}{\tau_d} \quad (4)$$

where k_1 is the scavenging rate of ^{234}Th. There are different relationships between k_1 and the POC con-

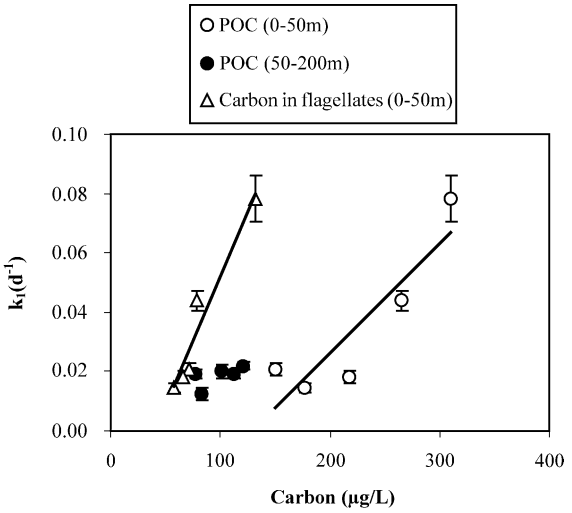

Fig. 4. Adsorption rate (k_1) versus flagellates (open triangle) and total carbon concentrations in suspended particles (open and closed circle corresponds to samples at 0–50 and 50–200 m, respectively). The carbon and k_1 values are averages of the upper 50 m and between 50 m and the deepest water samples.

centration in the surface and the deep water (Fig. 4). In the surface water (0–50 m), the scavenging rate of thorium onto suspended particles is correlated to the POC concentration in seawater. Below 50 m, the scavenging of thorium by resuspended particles is independent of POC, the lower content of which indicates that it is already partly remineralized. The scavenging of thorium is more efficient with high content of fresh organic carbon (Coale and Bruland, 1987). In the surface layer (0–50 m), flagellates represented 30–50% of the POC in suspension and we note that carbon in flagellates (P. Wassmann, unpublished data) correlate better with k_1 (Fig. 4) than with POC. It suggests that small phytoplankton cells play a key role in the thorium scavenging. Thorium forms strong complexes with carboxylated polysaccharides excreted by bacteria and phytoplankton that produce transparent exopolymer particles (TEP; Niven et al., 1997). Dissolved ^{234}Th complexation and subsequent aggregation of the exopolymers are suspected to be an important pathway for transferring ^{234}Th from solution up the particle size spectrum to sinking aggregates. *P. pouchetii* produces a large amount of TEP. However, the high *P. pouchetii* concentration at station 3 did not induce a very high scavenging rate of ^{234}Th.

4.3. Calibration of sediment trap with ^{234}Th

The loss of ^{234}Th from surface waters is a direct indication of the removal rate of material on sinking particles from the upper ocean (Coale and Bruland, 1985). In recent investigations, it became clear that the predicted ^{234}Th fluxes from the water column data and those measured in drifting sediment traps often disagree, by factors of 2–3 (Buesseler, 1991; Buesseler et al., 1994, 1995, 1998). In Bermuda Atlantic Time Series (BATS), Buesseler et al. (1994) concluded that upper sediment traps overcollect during low flux periods and undercollect during high flux periods. However, in the present study, the probably low current speed relative to the drifting traps and the absence of swimmers act as favourable factors to obtain a good efficiency of sediment traps. Assuming that the particulate matter flux is at steady state on time-scales of both the ^{234}Th tracer (~ 35 days) and the trap deployment (1 day), we can compare ^{234}Th fluxes measured on trap and model-derived ^{234}Th fluxes calculated at the same depth. These results are reported in Table 3. The ratio between ^{234}Th fluxes measured in traps and calculated by the steady-state model ranges from 0.7 to 1.7 with an average of 1.1. The lowest and largest ratios are observed at stations 2 and 3, respectively. However, the steady-state ^{234}Th model may not account for the bloom effect observed at station 3. When a bloom occurs, the total ^{234}Th activity decreases in response to the increasing export of particulate ^{234}Th and the steady-state model underestimates the export of particulate ^{234}Th. Excluding the station 3, the average ratio of the four remaining stations is 0.85 ± 0.15. It is not clear if the trapping efficiency lower than 100% reflects a loss of particle by the trap or if it is caused by a slight departure from the steady state. However, except for station 3, the comparison ^{234}Th fluxes data (traps and model) seem to be in agreement with steady state and minimizes the role of horizontal transport described in Section 4.2. Similarly, preliminary data collected in the Baltic Sea show a good agreement between fluxes obtained from the traps and fluxes calculated from ^{234}Th scavenging in the water column (Andersson et al., 2000).

The fact that swimmers were not observed could be a direct consequence of the traps not being poisoned.

Table 3
^{234}Th, POC fluxes data from sediment traps versus model and POC/^{234}Th$_p$ ratio in traps

Station	Trap depth (m)	^{234}Th flux in trap (dpm m^{-2} day^{-1})	^{234}Th flux in model (dpm m^{-2} day^{-1})	Ratio ^{234}Th flux (trap/model)	POC in trap (mmol m^{-2} day^{-1})	POC/^{234}Th$_p$ (μmol dpm^{-1})	POC model derived (mmol m^{-2} day^{-1})
St1	120	2118 ± 116	2053 ± 177	1.0	7.3	3.4	7.0 ± 0.7
St2	150	2074 ± 113	2900 ± 236	0.7	9.5	4.6	13.3 ± 1.3
St3	90	1814 ± 99	1050 ± 163	1.7	16.6	9.2	9.6 ± 1.6
St4	150	4147 ± 227	4857 ± 202	0.9	22.1	5.3	25.8 ± 1.8
St5	200	4713 ± 258	5037 ± 396	0.9	19.8	4.2	21.1 ± 2.0

Poisoned and unpoisoned drifting traps were never compared in the Barents Sea. However, the good agreement between the ^{234}Th fluxes measured in traps and estimated by model suggests that swimmers did not remove ^{234}Th contained in the trapped material. In some cases, sediment trap data can be flawed by trapping efficiency problems (Gardner, 1996), but in the present study, there is a remarkable agreement between trap and model fluxes (as compared to previously reported differences between the thorium method and traps). We suggest that it is possible to measure accurately particulate matter fluxes with short time deployed and unpoisoned sediment traps in a Lagrangian manner.

4.4. Vertical flux of particulate organic carbon and the POC/$^{234}Th_p$ ratio

Based on the scavenging model of ^{234}Th described above, the export flux of POC (P_{POC}) from the euphotic layer (50 m) can be estimated using the ^{234}Th deficit integrated between 0 and 50 m and POC/$^{234}Th_p$ ratio (Buesseler et al., 1992):

$$P_{POC} = \frac{POC}{^{234}Th_p} \times \lambda \int_0^{50} (A_U - A_{Th}) dz \quad (5)$$

In Section 4.3, we showed that our traps had a good trapping efficiency. If POC and ^{234}Th are carried by different types of particles, there is no guarantee that the result obtained with ^{234}Th can be extended to POC. However, we have reason to believe that there is a strong coupling between particles carrying ^{234}Th and POC along the transect. In this study, trap data are available to estimate POC fluxes. When trap data are not available, POC fluxes must be estimated based on the ^{234}Th/^{238}U disequilibrium and on the POC/$^{234}Th_p$ ratio of the sinking particulate matter. In this case, uncertainties on POC/$^{234}Th_p$ ratio are very important. Traditionally, the POC/$^{234}Th_p$ ratio of suspended particles (>0.2–1 μm) is used. However, suspended particles are not representative of the rapidly sinking particles that are responsible for the majority of particle export from the upper ocean (Charette et al., 1999; Michaels and Silver, 1988). Numerous studies suggest that the POC/$^{234}Th_p$ ratio of particulate matter decreases when particle size increases (Buesseler et al., 1995; Moran et al., 1993). This change in POC/$^{234}Th_p$ ratio may reflect the phytoplankton community because large phytoplankton cells (such as diatoms) have greater POC/$^{234}Th_p$ ratios than smaller cells (Charette et al., 1999). More recently, the use of in situ pumps allowed to collect large filtered particles (>53 μm). In the equatorial Pacific Ocean, POC/$^{234}Th_p$ ratios measured with in situ pump samples ranged from 0.5 to 4.5 μmol dpm^{-1} (Bacon et al., 1996; Buesseler et al., 1995; Murray et al., 1996). In the subtropical and equatorial Atlantic Ocean, POC/$^{234}Th_p$ ratios ranged from 10 to 35 μmol dpm^{-1} (Charette and Moran, 1999). Only a few studies allow a direct comparison between suspended and sinking particles. During the North Atlantic Bloom Experiment (NABE) experiment, POC/$^{234}Th_p$ ratios in traps were lower than POC/$^{234}Th_p$ ratios in suspended particles (>1 μm; Buesseler et al., 1992) while in the subarctic northeast Pacific Ocean, POC/$^{234}Th_p$ ratios in traps were higher than POC/$^{234}Th_p$ ratios in suspended particles (>1 μm; Charette et al., 1999). In the central equatorial Pacific, POC/$^{234}Th_p$ ratios of trapped particles ranged from 2.5 to 7 μmol dpm^{-1} and were three times higher than the ratios observed on large filtered particles (>53 μm; Murray et al., 1996). There are thus uncertainties on which POC/$^{234}Th_p$ ratio to use because traps with a low collection efficiency may discriminate among particles with different POC/$^{234}Th_p$ ratios.

The present study provides a new opportunity to compare POC/$^{234}Th_p$ ratios between small (suspended) and trapped particles (Tables 3 and 4). Suspended POC data were determined using 0.7 μm GF/F filters (Wassmann, 1991) and particulate ^{234}Th using 0.6 μm Nuclepore filters. We do not think that this difference can strongly alter the POC/$^{234}Th_p$ ratio of small filtered particles. From the sea surface to the depth of the trap, the average of POC/$^{234}Th_p$ ratio in suspended particles was 52.0 ± 9.9 μmol dpm^{-1}. The POC/$^{234}Th_p$ ratio in the traps ranged from 3.4 to 9.2 μmol dpm^{-1} (average 5.3 ± 2.2 μmol dpm^{-1}). POC/$^{234}Th_p$ ratios in suspended particles (>0.6 μm) are thus 4 to 16 times higher than those measured in traps. This difference of POC/$^{234}Th_p$ ratio between suspended and trapped particles remains to be explained.

There are several sources of primary organic matter in the Arctic Ocean: sea-ice algae, phytoplankton and terrestrial organic matter (Schubert and

Table 4
Particulate organic carbon, particulate ^{234}Th integrated from 0 to 50 m and 150–200 m and calculated POC fluxes based on POC/^{234}Th$_p$ ratio of small particles

Station	Depth range (m)	POC (10^3 μmol m^{-2})	^{234}Th$_p$ (10^3 dpm m^{-2})	POC/^{234}Th$_p$ (μmol dpm^{-1})	POC flux (mmol m^{-2} day^{-1})
St1	0–50	625	8.8 ± 0.4	71.2 ± 3.5	64.7 ± 8.1
	0–120	1077	19.7 ± 0.7	54.7 ± 2.0	112.3 ± 10.5
St2	0–50	909	9.2 ± 0.5	98.4 ± 4.8	81.4 ± 11.2
	0–150	1842	35.7 ± 1.1	51.7 ± 1.7	149.8 ± 13.1
St3	0–60	735	15.5 ± 1.0	47.6 ± 3.1	29.2 ± 6.4
	0–90	1010	26.9 ± 1.2	37.5 ± 1.6	39.4 ± 6.3
St4	0–50	1294	18.9 ± 0.8	68.4 ± 3.0	106.0 ± 7.5
	0–150	2401	47.2 ± 1.5	50.8 ± 1.6	247.0 ± 12.9
St5	0–50	1106	15.5 ± 0.7	71.4 ± 3.1	91.3 ± 7.1
	0–200	2378	36.5 ± 1.2	65.1 ± 2.2	327.7 ± 27.9

Calvert, 2001). In this study, phytoplankton carbon (PPC) represented most of the POC in the suspended matter while carbon in fecal pellets (FPC) and detritus in the suspended material represented a small fraction of the POC (FPC represented ~1–2% of the POC in suspension). This suggests that suspended particles contained a lot of labile POC (i.e. easily degradable). In the photic layer, we noted a predominance of flagellates in the standing stock except at station 3 where *P. pouchetii* were more abundant. Flagellates are not considered important for the vertical carbon flux due to their small size and low sinking rate (Reigstad, 2000). We assume that particles in suspension were aggregated and/or grazed by zooplankton and transformed into larger particles. During grazing and bacterial degradation of large aggregates, carbon is preferentially remineralized over ^{234}Th as thorium is not sensitive to particle mineralization (Arraes-Mescoff et al., 2001; Fisher et al., 1987). ^{234}Th tends to be enriched in pellet material, compared with bulk POC (Coale, 1990). This would lead to a strong decrease of the POC/^{234}Th$_p$ ratio in the large particles (pellets, aggregates) compared to small particles.

In this study, FPC represents from 20% to 50% of the POC in trapped particles except at station 3 where FPC was smaller with a predominance of *Phaeocystis* and flagellates. During the spring bloom, Andreassen and Wassmann (1998) have observed in sediment traps that only a small fraction of intact phytoplankton (i.e. ungrazed) reached deep waters (due to retention by grazers) and that the vertical flux of biogenic matter to deep waters was dominated by fecal matter. This suggests that trapped particles are enriched in pellets and aggregates compared to plankton cells (labile POC) and it could explain low values of POC/^{234}Th$_p$ ratios measured in traps.

If we use the thorium export flux and the POC/^{234}Th$_p$ ratio in suspended particles which ranges from 37.5 to 65.1 μmol dpm^{-1} (average 52.0 ± 9.9 μmol dpm^{-1}) between the sea surface and the sediment trap depth to determine the POC export, like in previous studies, we overestimate POC flux measured in traps at 90–200 m from 2 to 16 times. When we consider the POC/^{234}Th$_p$ ratio of the trapped

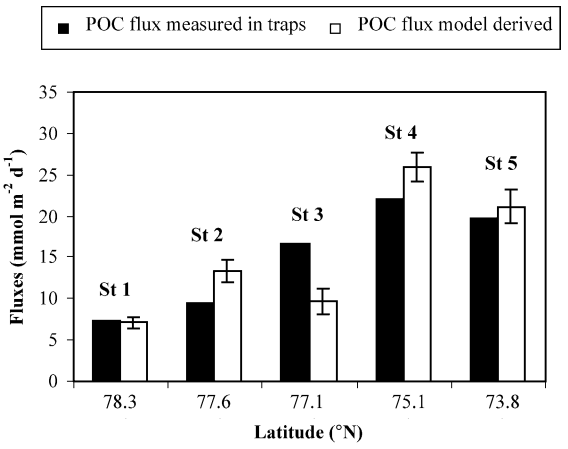

Fig. 5. Model-derived POC fluxes and POC fluxes measured in traps at 90–200 m (Eq. (5)).

Table 5
^{234}Th-derived POC fluxes in the Arctic Ocean

Zone	POC/$^{234}Th_p$ (μmol dpm^{-1})	POC fluxes (mmol m^{-2} d^{-1})	Author
Northeast Water Polynya	47	12–45	Cochran et al. (1995)
Central Arctic Ocean	13	0.3–7	Moran et al. (1997)
Chukchi Shelf	67	38	
Beaufort Sea	10	0.7–7	Moran et al. (2000)
Barents Sea	5 (sediment traps)	7–26	Coppola et al. (this study)
	50 (suspended particles)	55–255	

material for the calculation, our estimates are consistent with POC fluxes measured in traps. We do not suspect a collection efficiency problem in our study. At 150 m, the average of POC export calculated with ^{234}Th scavenging model is 15.4 ± 7.9 mmol C m^{-2} day^{-1} compared to 15.1 mmol C m^{-2} day^{-1} collected in traps (Fig. 5). The average of POC export flux over the five long stations is comparable with vertical carbon flux data simulated by Wassmann and Slagstad (1993). In this model, the average of POC flux along the same transect in the Barents Sea during the years 81, 82 and 83 in July at 75 m depth was 16.7 mmol C m^{-2} day^{-1}. The new production calculated by the nutrients depletion in the central Barents Sea in July 1999 varied from 57 mmol C m^{-2} day^{-1} in the ice-covered waters to 70 mmol C m^{-2} day^{-1} at the Polar Front with an average of 220 mmol C m^{-2} day^{-1} in the open waters south of the Polar Front (Reigstad et al., accepted for publication). It represents 9–20% of the POC fluxes collected by the sediment traps. This difference is maybe due to a remineralization process during the sampling cruise.

Although the average of ^{234}Th-derived POC fluxes reported in this study is comparable to other ^{234}Th-derived data obtained in the Arctic Ocean (Table 5), it appears that the highest rates of the previous studies are due to the high POC/$^{234}Th_p$ ratios measured on suspended particles in the Northeast Water Polynya (Cochran et al., 1995) and in the Chukchi Shelf (Moran et al., 1997). The POC/$^{234}Th_p$ ratio measured at the Northeast Water Polynya and Chukchi Shelf are as high as the POC/$^{234}Th_p$ ratio in suspended particles measured in the present study, so we cannot exclude that these fluxes are overestimated (as we would have overestimated the POC fluxes if we had considered the POC/$^{234}Th_p$ ratio of suspended particles).

5. Conclusion

Measurements of ^{234}Th depth profiles in the Barents Sea indicate that ^{234}Th/^{238}U disequilibrium is present in July in the entire sampling area. This is due to the high concentrations of biogenic matter in the water column. The ^{234}Th method confirms the accuracy of sediment traps in the Barents Sea. This allows to compare POC fluxes estimated with ^{234}Th model and measured POC fluxes in sediment traps. We suggest that high POC fluxes previously reported in the Arctic Ocean during the summer based on high POC/$^{234}Th_p$ ratios measured on suspended particles have been overestimated. We could not have reached our conclusion without a simultaneous measurement of POC and ^{234}Th in suspended and trapped particles. The discrepancy in POC/^{234}Th ratios between trap and suspended particles in this study is clear evidence that further knowledge of interactions of ^{234}Th with marine organic matter and fecal pellets is necessary to improve understanding of factors controlling the POC/^{234}Th ratio in the ocean and the vertical export of carbon (Andersson et al., 2000). We conclude that at present, we have to know the POC/^{234}Th ratios of the sinking matter (sediment trap material or large filtered particles) to quantify the POC export from ^{234}Th fluxes.

Acknowledgements

It is a pleasure to acknowledge the sedimentation group of the Norwegian College of Fishery Science in Tromsø. We are specially grateful to C. Wexels Riser, C. Svensen and M. Reigstad for their cooperation and assistance during the cruise ALV3 and the visit of L. Coppola during 1 month in the lab. We thank F. Lyard

for sharing his expertise for the barotropic calculations. We wish also to acknowledge the officers and the crew of the R/V Jan Mayen for their efforts in sampling. J. Dunne, M. Rutgers van der Loeff and an anonymous reviewer are thanked for these thoughtful comments. Thanks to K. Olli for providing unpublished phytoplankton data.

Associate editor: Dr. Robert F. Anderson

References

Andersson, P.S.Ö.G., Roos, P., Broman, D., Toneby, A., 2000. Particle mediated surface water export: comparison of estimates from ^{238}U–^{234}Th disequilibria and sediment traps in a continental shelf region. AGU Ocean Science Meeting, San Antonio, TX.

Andreassen, I.J., Wassmann, P., 1998. Vertical flux of phytoplankton and particulate biogenic matter in the marginal ice zone of the Barents Sea in May 1993. Mar. Ecol., Prog. Ser. 170, 1–14.

Arraes-Mescoff, R., et al., 2001. The behavior of Al, Mn, Ba, Sr, REE and Th isotopes during in vitro degradation of large marine particles. Mar. Chem. 73, 1–19.

Bacon, M.P., Rutgers van der Loeff, M.M., 1989. Removal of thorium-234 by scavenging in the bottom nepheloid layer of the ocean. Earth Planet. Sci. Lett. 92, 157–164.

Bacon, M.P., Cochran, J.K., Hirschberg, D., Hammar, T.R., Fleer, A.P., 1996. Export flux of carbon at the equator during EqPac time-series cruises estimated from ^{234}Th measurements. Deep-Sea Res., Part II 43, 1133–1153.

Buesseler, K.O., 1991. Do upper-ocean sediment traps provide an accurate record of particle flux? Nature 353, 420–423.

Buesseler, K.O., Bacon, M., Cochran, J.K., Livingston, H.D., 1992. Carbon and nitrogen export during the JGOFS North Atlantic Bloom Experiment estimated from ^{234}Th:^{238}U disequilibria. Deep-Sea Res. 39, 1115–1137.

Buesseler, K.O., Michaels, A.F., Siegel, D.A., Knap, A.H., 1994. A three dimensional time-dependent approach to calibrating sediment trap fluxes. Glob. Biogeochem. Cycles 8 (2), 179–193.

Buesseler, K.O., Andrews, J.A., Hartman, M.C., Belastock, R., Chai, F., 1995. Regional estimates of the export flux of particulate organic carbon derived from thorium-234 during the JGOFS EQPAC Program. Deep-Sea Res., Part II 42 (2–3), 777–804.

Buesseler, K.O., et al., 1998. Upper ocean export of particulate organic carbon in the Arabian Sea derived from thorium-234. Deep-Sea Res. 45, 2461–2487.

Charette, M.A., Moran, S.B., 1999. Rates of particle scavenging and particulate organic carbon export estimated using ^{234}Th as a tracer in the subtropical and equatorial Atlantic Ocean. Deep-Sea Res., Part II 46, 885–906.

Charette, M.A., Moran, S.B., Bishop, J.K.B., 1999. ^{234}Th as a tracer of particulate organic carbon export in the subarctic northeast Pacific Ocean. Deep-Sea Res., Part II 46, 2833–2861.

Chen, J.H., Edwards, R.L., Wasserburg, G.J., 1986. ^{238}U–^{234}U and ^{232}Th in seawater. Earth Planet. Sci. Lett. 80, 241–251.

Coale, K.H., 1990. Labyrinth of doom: advice to minimize the ''swimmer'' component in sediment trap collections. Limnol. Oceanogr. 35 (6), 1376–1381.

Coale, K.H., Bruland, K.W., 1985. ^{234}Th:^{238}U disequilibria within the California current. Limnol. Oceanogr. 30, 22–33.

Coale, K.H., Bruland, K.W., 1987. Oceanic stratified euphotic zone as elucidated by ^{234}Th:^{238}U disequilibria. Limnol. Oceanogr. 32, 189–200.

Cochran, J.K., Barnes, C., Achman, D., Hirschberg, D.J., 1995. Thorium-234/Uranium-238 disequilibrium as an indicator of scavenging rates and particulate organic carbon fluxes in the Northeast Water Polynya Greenland. J. Geophys. Res. 100-C3, 4399–4410.

Falk-Petersen, S., et al., 2000. Physical and ecological processes in the marginal ice zone of the northern Barents Sea during the summer melt period. J. Mar. Syst. 27, 131–159.

Fisher, N.S., Teyssié, J.-L., Krishnaswami, S., Baskaran, M., 1987. Accumulation of Th, Pb, U and Ra in marine phytoplankton and its geochemical significance. Limnol. Oceanogr. 32, 131–142.

Gardner, W.D., 1996. Sediment trap technology and sampling in surface waters. Report of the sediment trap workshop, 1st International JGOFS Symposium, Villefrance sur mer, France, May 8–12, 1995, 32 pp.

Legendre, L., 1990. The significance of microalgal blooms for fisheries and for the export of particulate organic carbon in oceans. J. Plankton Res. 12, 681–699.

Loeng, H., 1991. Features of the physical oceanographic conditions on the Barents Sea. Polar Res. 10 (1), 5–18.

Loeng, H., Ozhigin, V., Adlandsvik, B., 1997. Water fluxes through the Barents Sea. ICES J. Mar. Sci. 54, 310–317.

Luchetta, A., Lipizer, M., Socal, G., 2000. Temporal evolution of primary production in the central Barents Sea. J. Mar. Syst. 27, 177–193.

Michaels, A.F., Silver, M.W., 1988. Primary production, sinking fluxes and the microbial food web. Deep-Sea Res. 35, 473–490.

Moran, S.B., Smith, J.N., 2000. ^{234}Th as a tracer of scavenging and particle export in the Beaufort Sea. Cont. Shelf Res. 20, 153–167.

Moran, S.B., et al., 1993. Regional Variability in Size-Fractioned C/^{234}Th Ratios in the Upper Ocean: Importance of Biological Recycling. The Oceanography Society, Seattle, WA.

Moran, S.B., Ellis, K.M., Smith, J.N., 1997. ^{234}Th/^{238}U disequilibrium in the Central Arctic Ocean: implications for particulate organic carbon export. Deep-Sea Res., Part II 44 (8), 1593–1606.

Murray, J.W., et al., 1996. Export flux of particulate organic carbon from the central equatorial Pacific determined using a combined drifting trap-^{234}Th approach. Deep-Sea Res., Part II 43, 1095–1132.

Niven, S.E.H., Keplay, P.E., Budgen, J.B.C., 1997. The role of TEP in ^{234}Th scavenging during a coastal diatom bloom. In: Germain, P., Guary, J.C., Guéguéniat, P., Métivier, H. (Eds.), Radionuclides in the Oceans RADOC 96–97. Proceedings Part 1: Inventories, Behavior and Processes. Revue de la société Française de Radioprotection, Cherbourg-Octeville (France), pp. 213–218.

Okubo, K., 1971. Oceanic diffusion diagrams. Deep-Sea Res. 18, 789–802.

Olli, K., Wexels Riser, C., Wassmann, P., Ratkova, T., Arashkevich, E., Pasternak, A., 2002. Seasonal variation in vertical flux of biogenic matter in the marginal ice-zone and the central Barents Sea. J. Mar. Syst. (In press).

Reigstad, M., 2000. Thesis: Plankton community and vertical flux of biogenic matter in the north Norwegian fjords: regulating factors, temporal and spatial variations. University of Tromsø, Tromsø, Norway, 88 pp.

Reigstad, M., Wassmann, P., Riser, C.W., Øygarden, S., Rey, F., 2002. Seasonal variation in hydrography, nutrients and suspended biomass in the marginal ice-zone and the central Barents Sea. J. Mar. Syst. (accepted for publication).

Roy-Barman, M., Chen, J.H., Wasserburg, G.J., 1996. ^{230}Th–^{232}Th systematics in the central Pacific Ocean: the sources and the fates of thorium. Earth Planet. Sci. Lett. 139, 351–363.

Rutgers van der Loeff, M.M., Moore, W.S., 1999. Determination of natural radioactive tracers. Methods of Seawater Analysis, Chap. 13, 3rd ed. Verlag Chemie, Weinheim, pp. 365–397.

Schubert, C.J., Calvert, S.E., 2001. Nitrogen and carbon isotopic composition of marine and terrestrial organic matter in Arctic Ocean sediments: implications for nutrient utilization and organic matter composition. Deep-Sea Res., Part I 48, 789–810.

Slagstad, D., Wassmann, P., 1997. Climate change and carbon flux in the Barents Sea: 3-D simulations of ice-distribution, primary production and vertical export of particulate organic matter. Mem. Natl. Inst. Polar Res., Spec. Issue 51, 119–141.

Smetacek, V., et al., 1984. Seasonal stages characterizing the annual cycle of an inshore pelagic system. Rapp. P.-V. Reun. - Cons. Int. Explor. Mer. 183, 126–135.

Wassmann, P., 1991. Sampling and analysis of marine particles with PEBENOCO (Pelagic–Benthic Coupling in the Norwegian Coastal Zone), University of Tromsø, Norway. Marine Particles: Analysis and Characterization. American Geophysical Union, Washington, DC, pp. 97–99.

Wassmann, P., Slagstad, D., 1993. Seasonal and annual dynamics of particulate carbon flux in the Barents Sea. Polar Biol. 13, 363–372.

Wassmann, P., et al., 1999. Spring bloom development in the Marginal Ice Zone and the central Barents Sea. Mar. Ecol. 20 (3–4), 321–346.